Dielectric Relaxation of H-Bonded Liquids. Mixtures of Ethanol and *n*-Hexanol at Different Compositions and Temperatures

P. Petong, R. Pottel, and U. Kaatze*

Drittes Physikalisches Institut, Georg-August-Universität, Bürgerstr. 42-44, D-37073 Göttingen, Germany

Received: March 26, 1999; In Final Form: May 24, 1999

At different temperatures T (0 °C ≤ T ≤ 60 °C) and mole fractions x of ethanol ($0 \le x \le 1$) the complex (electric) permittivity of ethanol/*n*-hexanol mixtures has been measured as a function of frequency ν between 1 MHz and 18 GHz. Within this frequency range of measurement the dielectric spectra reveal two relaxation regions. The relaxation time of the dominating relaxation process varies between $\tau_1 = 63$ ps ($x = 1$; 60 °C) and $\tau_1 = 2.8$ ns ($x = 0$; 0 °C). The relaxation time τ_2 of the second process is smaller (5 ps ≤ τ_2 ≤ 109 ps). The extrapolated static permittivity $\epsilon(0)$ of the alcohol systems is evaluated to show that there is a noticeable effect of permanent electric dipole orientation correlation. The relaxation terms are discussed in the light of hydrogen bond fluctuations and modes of reorientational motions of alcohol molecules. A remarkable result is the finding that the activation enthalpy associated with the dominating relaxation process can be represented by a sum of contributions from interactions between the hydrogen bonding OH-groups and between the methylene as well as methyl groups of the alcohol molecules. This finding suggests intermolecular interactions between the aliphatic groups to play a siginificant role in the dynamics of the molecular reorientations.

1. Introduction

In recent years there has been a substantial change in our view of the molecular dynamics of hydrogen bonded liquids. In particular computer simulation studies have revealed valuable insights into fine details of the molecular reorientation process, also displaying some uniform aspects of relaxation mechanisms in associating liquids. Some global trends in the predictions from computer simulations have been verified by dielectric spectroscopy. Water at room temperature may be taken as an example to explain the scenario as resulting from the computer studies.

At room temperature most water molecules are associated, forming a random macroscopic hydrogen bond network well above the percolation threshold.[1−4] The bond strength fluctuates rapidly with correlation times as small as 0.1 to 1 ps. Reorientation of a molecule through a significant angle, however, occurs only if two preconditions are simultaneously fulfilled. First, the angular distribution of potential barries has to be flattened so that rotation of the molecule by thermal activation is facilitated. In addition, an appropriate site for the formation of a new hydrogen bond has to be offered. Both requirements for a significant reorientational motion are provided by the presence of an additional neighbor molecule, e.g., in the predominantly tetrahedrally coordinated water a fifth neighbor has to be present.[5] On normal conditions a considerable fraction of the water molecules is indeed fivefold or even sixfold coordinated.[6] Nevertheless, it takes about 10 ps (298 K) until favorable conditions for a reorientation of a given molecule exist.[1] The reorientational motion itself resembles a switching process, as it occurs within a short period of about 0.1 ps.[1,2] An analogous model of the molecular reorientation process in alcohols has been suggested by Sagal.[7]

Generalized to also apply for associating liquids other than water, the computer simulation studies may be taken to consider the dielectric relaxation time to be mainly given by the time for which a molecule has to wait until favorable conditions for the reorientational motions exist.[1] Since such conditions are provided by a suitably located and oriented additional neighbor molecule, the dielectric relaxation time τ of associating liquids is expected to depend on the number density of the hydrogen bonding sites within the liquid. The corresponding behavior has in fact been found for the normal monohydric alcohols and for mixtures of alcohols with water for which empirically the equation

$$\tau/\tau_w = \hat{\rho}^{-2.5} \tag{1}$$

relates the dielectric relaxation time τ to the normalized number density

$$\hat{\rho} = (c_w + cZ_\varphi)/c_{wo} \tag{2}$$

of hydrogen bonding sites.[8] In eq 1, τ_w denotes the dielectric relaxation time of pure water, in eq 2 c_w and c are the molar concentrations of water and of the nonaqueous constituent of the binary mixture, respectively, Z_φ is the number of hydrogen bonding groups per molecule of the nonaqueous constituent, and c_{wo} denotes the molar concentration of pure water at the temperature T.

Though the overall tendency on the τ data as constituted by eq 1 can be realized qualitatively, the physical basis of this relation is still unclear at the present. This is particularly true as the agreement between the measured data and the predictions from eq 1 is not perfect. Some systematic deviations of the experimental data for the long chain alcohols *n*-heptanol to *n*-decanol from the general trends in the τ values, for example, may be taken to indicate that factors other than the number density of hydrogen bonding sites might be important in influencing the molecular reorientation. We therefore decided to perform a systematic dielectric relaxation study of the system ethanol/*n*-hexanol as a function of composition and temperature.

10.1021/jp991046l CCC: $18.00
Published on Web 07/16/1999

TABLE 1: Density (ρ) as well as Concentrations of *n*-Hexanol (c_{C_6OH}) and Ethanol (c_{C_2OH}) of the Liquids at Different Temperatures (T) and Mole Fractions of C_2OH (x)

$T[K] \pm 0.05$	$x = 0$	$x = 0.357$	$x = 0.575$	$x = 0.819$	$x = 1$
		ρ kg/m^3 ± 1.5			
273.2	831.5	826.5	821.0	814.0	807.5
283.2	825.0	819.5	814.5	806.0	799.0
293.2	819.0	813.0	807.5	798.5	789.5
298.2	815.0	809.5	803.5	795.0	785.5
303.2	811.5	805.5	800.0	791.0	781.5
313.2	805.0	798.5	792.5	783.5	773.5
323.2	797.5	791.0	785.0	775.5	765.0
333.2	790.5	783.5	777.0	767.0	757.0
		c_{C_6OH} mol/L ± 0.02			
273.2	8.14	6.47	4.99	2.63	0
283.2	8.07	6.41	4.95	2.60	0
293.2	8.02	6.36	4.91	2.58	0
298.2	7.98	6.34	4.88	2.56	0
303.2	7.94	6.30	4.86	2.55	0
313.2	7.88	6.25	4.82	2.53	0
323.2	7.80	6.19	4.77	2.50	0
333.2	7.74	6.13	4.73	2.47	0
		c_{C_2OH} mol/L ± 0.02			
273.2	0	3.59	6.75	11.85	17.53
283.2	0	3.56	6.70	11.73	17.34
293.2	0	3.53	6.64	11.62	17.14
298.2	0	3.52	6.61	11.57	17.05
303.2	0	3.50	6.58	11.51	16.96
313.2	0	3.47	6.52	11.40	16.79
323.2	0	3.44	6.46	11.29	16.61
333.2	0	3.40	6.40	11.16	16.43

2. Experimental

2.1. Sample Liquids. Ethanol (abbreviated C_2OH) and *n*-hexanol (abbreviated C_6OH) have been used as delivered by the manufacturer (>99%, Merck, Darmstadt, Germany). Mixtures with mole fraction $x = 0.819$, 0.575, and 0.357 of ethanol have been obtained by weighing appropriate amounts of the constituents into suitable flasks.

2.2. Density. At temperatures between 273.2 K and 333.2 K the density ρ of the liquids has been measured to within 0.15% using a set of aerometers. At 298.2 K the ρ data have been verified pycnometrically. The densities of the liquids are displayed in Table 1. Also given in Table 1 are the molar concentrations of the alcohols as resulting from the density data.

2.3. Complex Permittivity Spectra. Between 1 MHz and 18 GHz the complex permittivity

$$\epsilon(\nu, T) = \epsilon'(\nu, T) - i\epsilon''(\nu, T) \qquad i = (-1)^{1/2} \qquad (3)$$

of the sample liquids has been measured as a function of frequency ν and temperature T using two different methods. From 1 MHz to 3 GHz a computer- controlled network analyzer (Hewlett-Packard 8753A), combined with a reflection test set (Hewlett-Packard 85044A), has been utilized to measure the input impedance of suitable specimen cells of the cutoff variety.[9] These cells essentially consist of a coaxial line/circular cylindrical waveguide transition containing the liquid. The diameter of the circular waveguide is sufficiently small to prevent wave propagation. In order to achieve maximum sensitivity in the measurements the length l of the piece of coaxial line filled with the sample can be matched to the permittivity of the liquid under test and also to a particular part of the frequency range. Different cell lengths l between 0 and 40 mm have been used. For each cell length four (frequency independent) cell parameters have to be known. These parameters have been determined by calibration measurements using the empty cells and the cells filled with suitable reference liquids. We used water, acetone, and ethyl acetate as reference. Comparison between sample permittivity data obtained from cells with different length and also from calibrations with different reference liquids, for most part of the frequency range (5 MHz $\leq \nu \leq$ 1 GHz), resulted in an error of 1% in both the ϵ' and ϵ'' values. Toward lower and higher frequencies the uncertainty in the permittivity data increases ($\Delta\epsilon'/\epsilon' = 0.02$, $\Delta\epsilon''/\epsilon'' = 0.03$ at 1 MHz $\leq \nu <$ 5 MHz; $\Delta\epsilon'/\epsilon' = 0.05$, $\Delta\epsilon''/\epsilon'' = 0.07$ at 1 GHz $< \nu \leq$ 3 GHz).

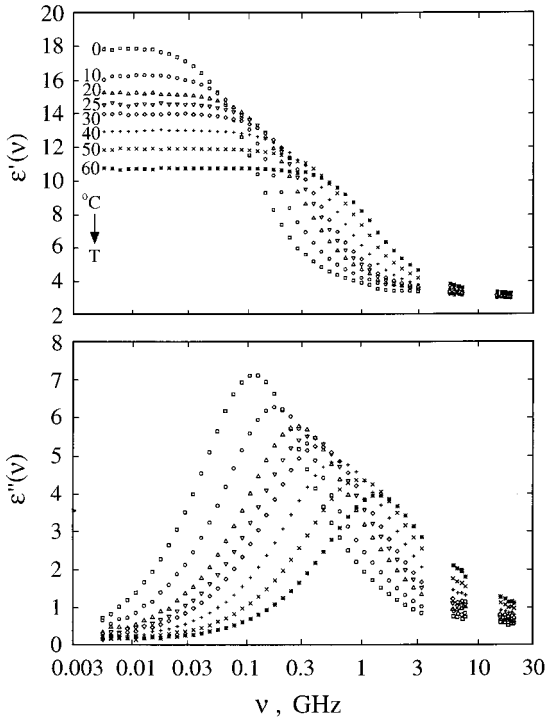

Figure 1. Real part ϵ' and negative imaginary part ϵ'' of the complex permittivity displayed versus frequency ν for an ethanol/*n*-hexanol mixture (mole fraction of ethanol $x = 0.357$) at different temperatures.

From 5.3 to 18 GHz we used automated waveguide systems to measure the complex permittivity of the liquids.[10] The transfer function of double beam interferometers, one branch of which was essentially formed by the specimen cell, matched to the respective frequency range, has been continuously recorded at varying cell length. The cells consisted of a piece of circular cylindrical waveguide filled with the liquid under test. Another circular waveguide was immersed in the liquid in order to probe the electromagnetic fields within the cell. With the aid of a high precision stepping motor drive, it was precisely shiftable along the direction of wave propagation. The errors in the permittivity data have been derived from repeated measurements as well as from a comparison of measured values for reference liquids to literature data and to such determined with a second set of microwave interferometers. Measurements with the latter apparatus have been performed by manually adjusting zero signal at the interferometer output. The error in the ϵ' and ϵ'' data determined with the automated interferometer method was smaller than 2% throughout.

In all measurements the error in the determination of the frequency of the electromagnetic signal was smaller than 0.1%. The temperature of the sample liquids was controlled to within 0.05 K.

3. Results and Treatment of Dielectric Spectra

In Figure 1 the dielectric spectra of a hexanol/ethanol mixture at the eight temperatures of measurement are shown. At all

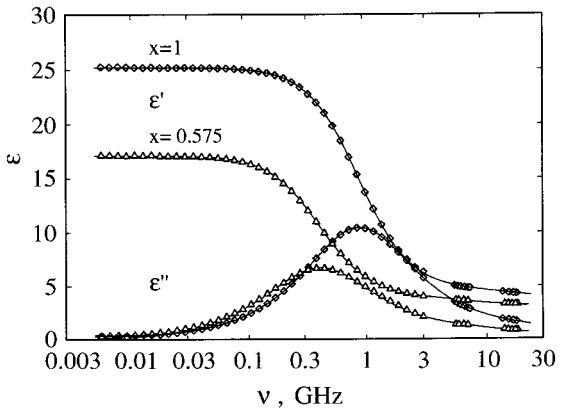

Figure 2. Complex dielectric spectra for ethanol ($x = 1$) and an ethanol/*n*-hexanol mixture ($x = 0.575$) at 20 °C. The curves are graphs of the spectral function defined by eq 4 with parameter values resulting from the fitting procedure (Tables 2, 3).

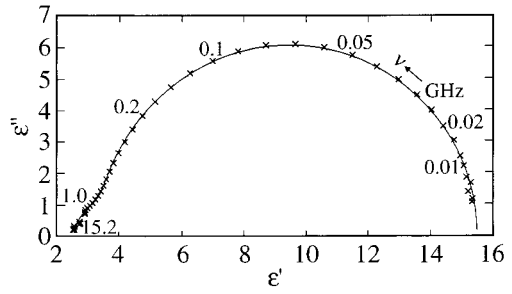

Figure 3. Complex plane representation of the dielectric spectrum for *n*-hexanol at 0 °C. The curve represents the spectral function eq 4 with the parameters given in Tables 2 and 3.

temperatures the spectra exhibit one discrete dispersion ($d\epsilon'(\nu)/d\nu < 0$)/dielectric loss ($\epsilon''(\nu) > 0$) region. According to our expectations the frequency ν_m of the relative maximum in the ϵ'' spectra noticeably increases and the extrapolated static permittivity $\epsilon(0) = \epsilon'(\nu \rightarrow 0)$ decreases with temperature. A plot of the complex dielectric spectra measured at different mixture compositions at 293.2 K is given in Figure 2. Both the relaxation frequency ν_m and static permittivity $\epsilon(0)$ decrease monotonuously with decreasing ethanol content.

The high frequency wings ($\nu > \nu_m$) of the ϵ' as well as ϵ'' spectra appear to be somewhat deformed as compared to a Debye-type relaxation spectrum with one discrete relaxation time. This finding is more obviously illustrated by Figure 3 where a complex plane representation of the dielectric spectrum of *n*-hexanol is given at 273.2 K. The deformed arc constituted by the permittivity data is in conformity with the assumption that spectra of alcohols reflect a sum of Debye relaxation terms[11−13] which is widely accepted now.[14−20] Inspection of microwave permittivity spectra up to 89 GHz,[17,20] particularly of spectra that additionally include far-infrared data,[17] resulted in a consistent description of the measured data in terms of a superposition of three relaxation terms with discrete relaxation time. However, for ethanol, for example, the relaxation time τ_3 of the fastest relaxation process at 25 °C is as small as 1.8 ps,[17] corresponding with a relaxation frequency of about 90 GHz. Also small is the relaxation amplitude $\Delta\epsilon_3$ (= 1.1) of the high frequency relaxation term as compared to the total relaxation amplitude $\epsilon(0) - \check{\epsilon}(\infty) = \Delta\epsilon_1 + \Delta\epsilon_2 + \Delta\epsilon_3 = 21.6$ at 25 °C.[17] Here $\check{\epsilon}(\infty)$ denotes the extrapolated high-frequency permittivity and the $\Delta\epsilon_i$ ($i = 1, 2, 3$) are the dispersion steps of the Debye relaxation terms. Since we measured at frequencies up to 18 GHz only, it is sufficient to represent the dielectric relaxation of the alcohols and of their mixtures by a sum of just two Debye terms. Hence the spectral function

$$R(\nu) = R'(\nu) - iR''(\nu) = \epsilon(\infty) + \frac{\Delta\epsilon_1}{1 + i\omega\tau_1} + \frac{\Delta\epsilon_2}{1 + i\omega\tau_2} \quad (4)$$

has been used to analytically represent the measured spectra ($\epsilon(\infty) > \check{\epsilon}(\infty)$). This function has been fitted to the complex permittivity data by minimizing, with the aid of a Marquardt algorithm,[21] the reduced variance, defined by

$$\chi^2 = \frac{1}{N - P - 1}\sum_{n=1}^{N}\left[\left(\frac{R'(\nu_n) - \epsilon'(\nu_n)}{\Delta\epsilon'(\nu_n)}\right)^2 + \left(\frac{R''(\nu_n) - \epsilon''(\nu_n)}{\Delta\epsilon''(\nu_n)}\right)^2\right] \quad (5)$$

Here ν_n ($n = 1, ..., N$) denote the frequencies of measurement, $P = 5$ is the number of adjustable parameters of the model relaxation function ($\epsilon(\infty)$, $\Delta\epsilon_1$, τ_1, $\Delta\epsilon_2$, τ_2), and the $\Delta\epsilon'(\nu_n)$, $\Delta\epsilon''(\nu_n)$ are the experimental errors in the complex permittivity data. The uncertainties in the parameter values obtained from the nonlinear least-squares regression analysis have been derived from additional runs in which sets of pseudodata $\tilde{\epsilon}'(\nu_n)$, $\tilde{\epsilon}''(\nu_n)$ were considered in the fitting procedure. The $\tilde{\epsilon}'(\nu_n)$, $\tilde{\epsilon}''(\nu_n)$ data have been generated by adding, within the limits of experimental error, $\pm\Delta\epsilon'(\nu_n)$, $\pm\Delta\epsilon''(\nu_n)$, random values to the measured permittivity data.

The values for the parameters of the model relaxation function *R* are displayed in Tables 2 and 3. Examples of graphs of $R(\nu)$ (eq 4) with parameter values resulting from the fitting procedure are shown in Figures 2 and 3.

4. Discussion

4.1. Molar Volumes. Assuming the constituents to maintain their molar volumes Φ_{C_2OH} and Φ_{C_6OH} when mixed, the density of the mixtures can be calculated from the pure alcohol data

$$\rho_{ideal} = \frac{(M_{C_2OH} - M_{C_6OH})x + M_{C_6OH}}{(M_{C_2OH}/\rho_{C_2OH} - M_{C_6OH}/\rho_{C_6OH})x + M_{C_6OH}/\rho_{C_6OH}} \quad (6)$$

M_{C_2OH} and M_{C_6OH} denote the C_2OH and C_6OH molar weights, respectively, ρ_{C_2OH} and ρ_{C_6OH} are the densities of the pure liquids. As shown by the plot of densities in Figure 4, the ρ_{ideal} data as calculated according to eq 6, within the limits of experimental error, fit nicely to the measured ρ data. This is not a trivial result. With water/ethanol mixtures, for instance, significant differences between the ρ_{ideal} and the ρ data are found.[22,23] Disregarding any prospective compensation of unnoticed effects, we conclude that no changes in the molar volume occur when ethanol is added to *n*-hexanol. On these conditions it seems to be justified to assign the difference $\Phi_{C_6OH} - \Phi_{C_2OH}$ to the molar volume of the four extra $-CH_2-$ groups of *n*-hexanol. In Figure 5 the molar volume Φ_{CH_2} for a $-CH_2-$ group is displayed as a function of temperature. Quite reasonable values between 16.45 $cm^3\ mol^{-1}$ at 0 °C and 17.1 $cm^3\ mol^{-1}$ at 60 °C are found. These values compare with $\Phi_{CH_2} = 16.2\ cm^3\ mol^{-1}$ (25 °C) for a $-CH_2-$ group of an alkyl chain within a micellar core.[24]

4.2. High Frequency Permittivity. The extrapolated high frequency permittivity values $\epsilon(\infty)$ clearly exceed the squared optical index of refraction n^2 of the liquids. For C_2OH and C_6OH at 25 °C $n^2 = 1.85$ and 2.00, respectively.[25] The difference $\epsilon(\infty) - n^2$ is partly due to molecular vibrations and also librational motions of the hydrogen bonded network of alcohol

TABLE 2: Parameter Values of the Relaxation Function $R(\nu)$ Defined by Eq 4 for the Ethanol/*n*-Hexanol Mixtures at Different Compositions and Temperatures (*f*: Data Fixed at the Mean of the Values at Lower Temperatures)

$T[K]$ ±0.5	$x = 0.00$	$x = 0.357$	$x = 0.575$	$x = 0.819$	$x = 1$
			$\epsilon(\infty)$		
273.2	2.57 ± 0.05	2.77 ± 0.07	2.96 ± 0.06	3.25 ± 0.08	3.47 ± 0.10
283.2	2.67 ± 0.08	2.80 ± 0.07	2.98 ± 0.08	3.12 ± 0.10	3.37 ± 0.20
293.2	2.62 ± 0.07	2.77 ± 0.08	2.93 ± 0.07	3.30 ± 0.10	3.50 ± 0.10
298.2	2.61 ± 0.10	2.77 ± 0.08	2.89 ± 0.08	3.23 ± 0.10	3.40 ± 0.20
303.2	2.64 ± 0.10	2.71 ± 0.06	2.82 ± 0.10	3.23 ± 0.20	3.33 ± 0.20
313.2	2.56 ± 0.09	2.59 ± 0.10	2.75 ± 0.10	3.08 ± 0.10	3.28 ± 0.30
323.2	2.50 ± 0.08	2.61 ± 0.07	2.76 ± 0.20	2.92 ± 0.20	3.15 ± 0.30
333.2	2.39 ± 0.08	2.56 ± 0.08	2.57 ± 0.20	2.90 ± 0.20	3.10 ± 0.30
			$\Delta\epsilon_1$		
273.2	12.05 ± 0.04	14.31 ± 0.04	16.20 ± 0.08	19.61 ± 0.08	23.84 ± 0.10
283.2	10.51 ± 0.04	12.57 ± 0.05	14.31 ± 0.06	17.45 ± 0.04	22.19 ± 0.05
293.2	9.43 ± 0.04	11.52 ± 0.06	13.21 ± 0.06	15.89 ± 0.09	20.65 ± 0.07
298.2	8.94 ± 0.05	10.96 ± 0.06	12.67 ± 0.08	15.01 ± 0.05	20.02 ± 0.06
303.2	8.43 ± 0.06	10.40 ± 0.05	12.01 ± 0.09	14.31 ± 0.07	19.46 ± 0.10
313.2	7.54 ± 0.05	9.51 ± 0.03	10.99 ± 0.09	13.17 ± 0.08	18.05 ± 0.08
323.2	6.71 ± 0.08	8.41 ± 0.06	9.59 ± 0.06	12.14 ± 0.10	16.93 ± 0.10
333.2	5.73 ± 0.05	7.34 ± 0.06	8.58 ± 0.04	11.00 ± 0.09	15.60 ± 0.11
			$\Delta\epsilon_2$		
273.2	0.86 ± 0.06	0.81 ± 0.07	0.95 ± 0.06	1.00 ± 0.10	1.1 ± 0.10
283.2	0.83 ± 0.05	0.89 ± 0.06	0.99 ± 0.08	1.00 ± 0.10	1.1 ± 0.10
293.2	0.83 ± 0.06	0.85 ± 0.05	0.92 ± 0.08	1.00 ± 0.10	1.0 ± 0.10
298.2	0.81 ± 0.04	0.82 ± 0.04	0.84 ± 0.08	1.10 ± 0.10	1.1 ± 0.20
303.2	0.77 ± 0.08	0.84 ± 0.07	0.88 ± 0.07	1.16 ± 0.10	1.1 ± 0.10
313.2	0.78 ± 0.07	0.85 ± 0.09	0.88 ± 0.06	1.12 ± 0.20	1.1(*f*)
323.2	0.75 ± 0.06	0.84(*f*)	0.91(*f*)	1.04(*f*)	1.1(*f*)
333.2	0.83 ± 0.08	0.84(*f*)	0.91(*f*)	1.04(*f*)	1.1(*f*)

TABLE 3: Values for the Relaxation Times of the Model Spectral Function $R(\nu)$ Defined by Eq 4 for the Ethanol/*n*-Hexanol Mixtures at Different Compositions and Temperatures

$T[K]$ ±0.5	$x = 0.00$	$x = 0.357$	$x = 0.575$	$x = 0.819$	$x = 1$
			τ_1 ps		
273.2	2800 ± 8	1387 ± 5	849 ± 4	497 ± 4	310 ± 2
283.2	1724 ± 10	910 ± 5	581 ± 4	349 ± 2	233 ± 1
293.2	1061 ± 7	598 ± 2	395 ± 2	250 ± 1	184 ± 2
298.2	824 ± 4	479 ± 2	321 ± 2	217 ± 1	162 ± 2
303.2	673 ± 3	401 ± 3	276 ± 2	190 ± 2	143 ± 2
313.2	442 ± 5	278 ± 2	193 ± 1	138 ± 1	105 ± 1
323.2	286 ± 3	185 ± 1	140 ± 1	102 ± 1	82 ± 1
333.2	186 ± 1	126 ± 1	96 ± 1	77 ± 1	63 ± 1
			τ_2 ps		
273.2	109 ± 7	32 ± 6	27 ± 5	15 ± 4	6 ± 3
283.2	61 ± 6	30 ± 5	27 ± 5	11± 4	6 ± 3
293.2	46 ± 3	24 ± 3	21 ± 3	17 ± 4	8 ± 3
298.2	35 ± 3	23 ± 3	16 ± 3	15 ± 3	6 ± 3
303.2	33 ± 3	18 ± 2	14 ± 2	16 ± 3	7 ± 3
313.2	23 ± 2	12 ± 2	11± 2	13± 2	6 ± 3
323.2	15 ± 2	11 ± 2	11± 2	10± 2	5 ± 3
333.2	11 ± 2	9 ± 2	7 ± 2	9 ± 2	6 ± 3

molecules. Reorientational motions of non-H-bonded OH-groups[11,26] are assumed to additionally contribute a relaxation process at frequencies well above our range of measurements. At all temperatures considered in this study the $\epsilon(\infty)$ values increase with mole fraction x of C_2OH. This finding might be due, at least in part, to the increasing concentration of OH-groups. It might be also taken to indicate that the amount of temporarily unbound OH-groups decreases when going from ethanol to hexanol. It has to be kept in mind, however, that $\epsilon(\infty)$ is an intricate parameter in the dielectric spectra of associating liquids. Without reliable permittivity data in the far infrared region, $\epsilon(\infty)$ is only ill defined experimentally. In addition, extrapolation according to a Debye-type relaxation function leads to a wrong result as, from a fundamental point of view,[27] $\lim_{\nu\to\infty}[d\epsilon''(\nu)/d\epsilon'(\nu)] = -0$ should hold instead of $\lim_{\nu\to\infty}[d\epsilon''(\nu)/d\epsilon'(\nu)] = \infty$ as predicted by eq 4.

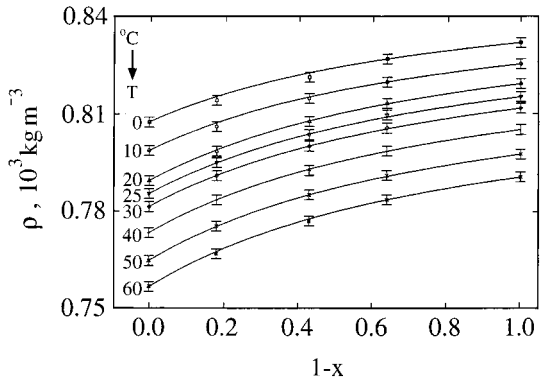

Figure 4. Density ρ of the ethanol/*n*-hexanol mixtures at different temperatures plotted versus the mole fraction $1 - x$ of *n*-hexanol. Full curves represent the predictions by eq 6.

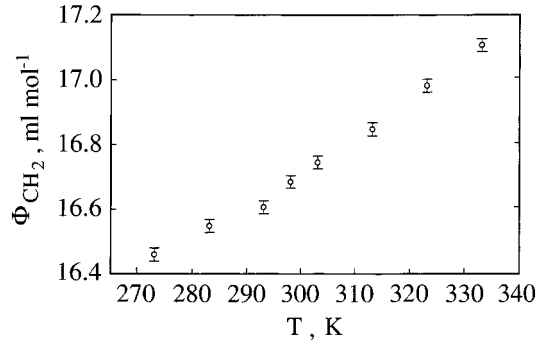

Figure 5. The molare volume Φ_{CH_2} of a CH_2 group in a normal alcohol, as resulting from our density data, displayed as a function of temperature.

4.3. Static Permittivity, Dipole Orientation Correlation. Below about 20−200 MHz (0−60 °C, respectively) the $\epsilon'(\nu)$ values of the liquids are nearly independent of frequency (Figure 1). Therefore, the extrapolated static permittivity values are well defined by the measurements and, within the limits of experi-

mental error $\Delta\epsilon(0)/\epsilon(0) = 2\%$, do not depend on the particular model relaxation function used to extrapolate the measured spectra toward $\nu = 0$. Also within the limits of error our $\epsilon(0)$ values for C_2OH and C_6OH agree with literature data measured at very low frequencies.[28−30] Any additional dispersion in $\epsilon'(\nu)$ at frequencies below our measuring frequency range can thus be excluded.

Within the present series of spectra the highest $\epsilon(0)$ value is found for ethanol at 0 °C ($\epsilon(0) = 28.4$, $x = 1$) and the smallest one for hexanol at 60 °C ($\epsilon(0) = 8.95$, $x = 0$). The obvious tendency of the extrapolated static permittivity to decrease with temperature T and with decreasing OH-group concentration c_{OH} is in accordance with the Fröhlich theory of the static permittivity of a dipolar liquid[31,32] which predicts

$$\epsilon(0) - \epsilon(\infty) = \frac{4\pi N_A}{3k_B T}\frac{3\epsilon(0)}{2\epsilon(0)+\epsilon_\infty}\left(\frac{\epsilon_\infty + 2}{3}\right)^2 g\mu^2 c_{OH} \quad (7)$$

Herein N_A is Avogadro's number, k_B the Boltzmann constant, ϵ_∞ a high frequency permittivity to be discussed below, g is the Kirkwood dipole orientation correlation factor,[33] and μ and c_{OH} are the molecular permanent electric dipole moment in the gaseous state and molar concentration, respectively, of the dipolar molecules.

For one-component systems, eq 7 allows to calculate the g factor from the low and high frequency permittivity data and to thus gain insights into the spatial correlations of dipole orientations. For mixtures of different dipolar species the situation is more complicated since a rigorous treatment of the static permittivity would involve various different dipole moment orientation correlations. In order to enable a clear analytical treatment of the static permittivity, irrespective of different types of molecular associates that might exist in the alcohole mixtures, we assume the dipolar COH-group orientation to be governed by one (effective) dipole correlation factor g only. As the dipole moment μ of normal alcohols in the gaseous state does not noticeably depend on the length of the hydrocarbon chain (methanol, $\mu = 1.70$ D;[34] *n*-heptanol, $\mu = 1.66$ D;[34] *n*-decanol, $\mu = 1.68$ D[35,36]) we use the same μ value (= 1.68 D) for both ethanol and *n*-hexanol here. Consequently, c_{OH} is identified with the concentration $c_{C_2OH} + c_{C_6OH}$ (Table 1). It is, however, still unclear which ϵ_∞ value has to be used in the Fröhlich model. We just know that ϵ_∞ should adopt a value somewhere between the squared optical refractive index n^2 and the permittivity $\epsilon(\infty)$ as extrapolated from the microwave spectra. Unfortunately, the g values calculated from eq 7 depend significantly on ϵ_∞. Let water at room temperature serve as an example. Using $\epsilon_\infty = \epsilon(\infty)$ with the permittivity data listed in ref 37 and with $\mu = 1.84$ D, $g < 1$ follows. Kirkwood, taking $\epsilon_\infty = n^2 = (1.33)^2$ found $g = 2.8$,[33] which would point at a substantial tendency toward equal alignment of dipole moments. Hill showed that $\epsilon_\infty = 4.3$ is in conformity with $g = 1$[38] which would suggest orientation correlations to be absent at all.

Being aware of the variance in the high frequency permittivity, we first used $\epsilon_\infty = \epsilon(\infty)$ (Table 2) in order to calculate minimum orientation correlation factors. The resulting $g = g_{\epsilon(\infty)}$ values for the ethanol/*n*-hexane mixtures of different composition and temperature are dispayed in Figure 6. Quite remarkably, in contrast to water at room temperature, the $g_{\epsilon(\infty)}$ values of the C_2OH/C_6OH system are substantially larger than 1. Hence without doubts there exists a preferential equal alignment of COH-group dipole moments in the alcohol molecular structures, assumed to be chainlike. While for ethanol and also for mixtures of high ethanol content $g_{\epsilon(\infty)}$ (=1.6) is found nearly independent

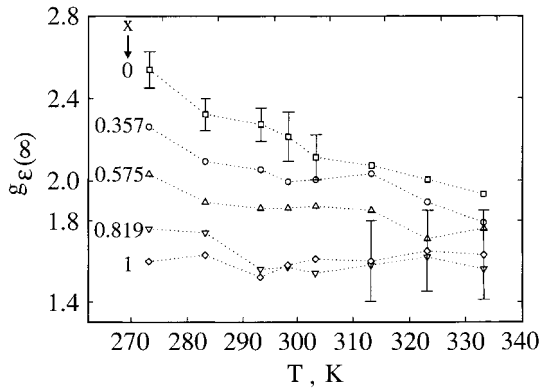

Figure 6. The minimum effective dipole orientation correlation factor $g_{\epsilon(\infty)}$ of the ethanol/*n*-hexanol mixtures of different composition plotted versus temperature T.

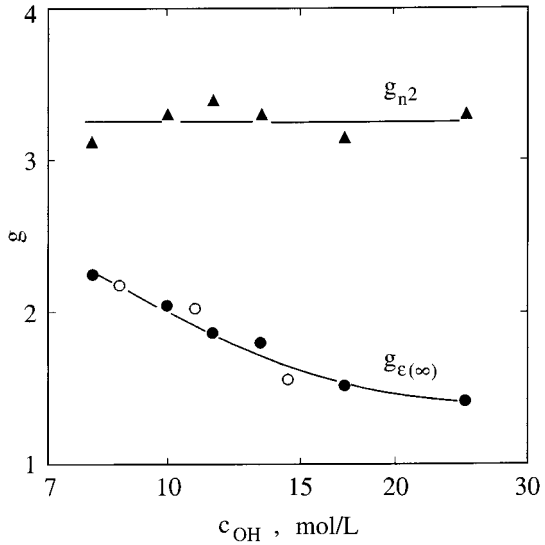

Figure 7. Minimum ($g_{\epsilon(\infty)}$, full points, circles) and maximum (g_{n^2}, triangles) values of the dipole orientation correlation factor versus concentration c_{OH} of dipolar groups for normal alcohols (full symbols) and for ethanol/*n*-hexanol mixtures (open symbols) at 20 °C.

of temperature T, $g_{\epsilon(\infty)}$ for mixtures rich of *n*-hexanol and for *n*-hexanol decreases with T. This finding suggests a lower degree of order in the high temperature liquid structure. The noticeable increase in the orientation correlation values when going from ethanol ($g_{\epsilon(\infty)} = 1.6$, 0 °C) to *n*-hexanol ($g_{\epsilon(\infty)} = 2.55$, 0 °C) is also shown by Figure 7 where correlation factor data at 20 °C are displayed as a function of OH-group concentration. Additionally given are $g_{\epsilon(\infty)}$ values for the series of normal alcohols $CH_3(CH_2)_{m-1}OH$ from methanol to hexanol at the same temperature. These data have been calculated using static permittivity data from the literature[30,39,40] assuming $\epsilon(\infty)$ of the alcohols to linearly decrease with m ($\epsilon(\infty) = 3.4$, $m = 2$; $\epsilon(\infty) = 2.61$, $m = 6$). The finding of $g_{\epsilon(\infty)}$ of the ethanol/*n*-hexane mixtures to decrease in a similar fashion with c_{OH} as within the series of normal alcohols may be taken to indicate a less strong liquid order at high OH-group concentration, that is at a high probability density for the formation of hydrogen bonds. However, this might be a hasty conclusion since an orientation correlation factor $g = g_{n^2}$ (= 3.3) independent of c_{OH} results (Figure 7), if $\epsilon = n^2$ is used in eq 6.

Even though no definite conclusion can be drawn on the dependence of g upon the OH-group concentration and the temperature, the existence of a substantial effect of dipole orientation correlation in the alcohol systems clearly follows from the static permittivity data.

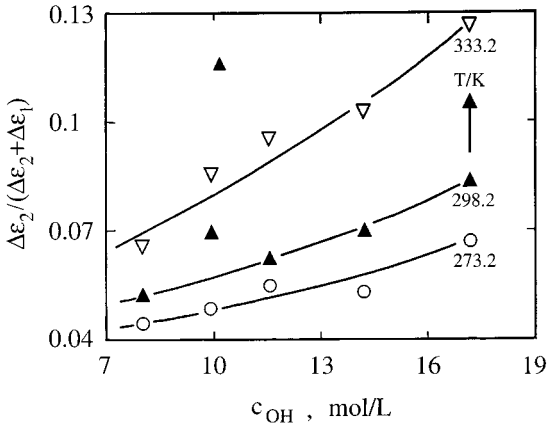

Figure 8. The relative contribution $\Delta\epsilon_2/(\Delta\epsilon_2 + \Delta\epsilon_1)$ of the high frequency relaxation to the total relaxation amplitude for the ethanol/*n*-hexanol mixtures at three temperatures displayed as a function of OH group concentration c_{OH}.

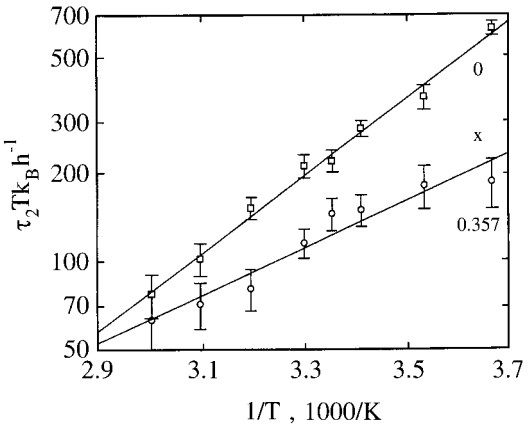

Figure 9. Eyring plot for the relaxation times τ_2 of the high frequency process for *n*-hexanol ($x = 0$) and an ethanol/hexanol mixture ($x = 0.357$).

4.4. High Frequency Relaxation. Within the limits of experimental error the amplitude $\Delta\epsilon_2$ of the high frequency relaxation process is independent of temperature and it increases slightly only with the OH-group concentration ($\Delta\epsilon_2 = 0.8$, C_6-OH; $\Delta\epsilon_2 = 1.1$, C_2OH; $0 \le T \le 60$ °C, Table 2). The relative contribution $\Delta\epsilon_2/(\Delta\epsilon_1 + \Delta\epsilon_2) = \Delta\epsilon_2/(\epsilon(0) - \epsilon(\infty))$ of the high frequency relaxation to the total dispersion step also increases with c_{OH} (Figure 8).

It is generally accepted now that in alcohols the relaxation of the non-H-bonded OH-group rotation around the C−O bond occurs at frequencies well above our measuring range. Relaxation times reported for this process are typically in the order of 1 ps (e.g., methanol, 25 °C[20]), corresponding with a relaxation frequency around 150 GHz. Hence the dielectric polarization due to these OH-group reorientational motions contributes to the $\epsilon(\infty)$ values of our spectra. Consequently, the relaxation denoted "high frequency" here may be assumed to reflect the over-all rotation of monomers, as originally suggested by Garg and Smyth.[11] To some extent this suggestion has been approved by the finding of dielectric relaxation times of relevant nonassociating liquids in the order of our τ_2 values. Particularly thiols[41] may serve as an example. For *n*-hexanethiol at 25 °C a relaxation time value of 33 ps has been derived from a Davidson−Cole evaluation[42] of the dielectric spectrum, whereas $\tau_2 = 35$ ps for C_6OH at the same temperature (Table 3). In the Davidson−Cole evaluation the relaxation time distribution parameter was $\beta = 0.45$, approximately corresponding with the two Debye relaxation times 18 ps and 2 ps.

However, computer simulation studies of methanol, ethanol, and *n*-propanol at 25 °C reveal a monomer content between 1.1 and 2 per cent of alcohol molecules only.[43] This concentration has been considered too small to account for the relaxation amplitude $\Delta\epsilon_2$ if only a monomer reorientation process is assumed. Barthel et al. suggested terminal molecules of the hydrogen bonded chainlike aggregates to add contributions to the high frequency relaxation process, due to reorientational motions around the directions of their hydrogen bond.[17] These motions resemble the monomer rotation but are restricted to a single axis.

We here, and in the case of the low frequency relaxation (section 4.5), assume the "wait-and-switch" model as briefly outlined in the Introduction to be applicable to the COH-dipole reorientational motion. According to this model an H-bonded dipolar group will switch its dipole orientation preferably if an additional neighbor molecule offers a suitable site for a new hydrogen bond. Following computer simulation studies of methanol,[44] the strength of the original H-bond decreases already when, within the course of thermal fluctuations, the new bonding site approaches the position under consideration. The motions of the additional neighbor molecule as well as the reorientation motions of the switching dipolar group are assumed to follow an activated jump mechanism. Hence according to the Eyring relation[45]

$$\tau_i = \frac{h}{k_B T} C_{fi} \times \exp(\Delta G_i^{\ddagger}/RT) \qquad i = 1, 2 \tag{8}$$

the relaxation times τ_i involved are governed by the Gibbs free energies of activation $\Delta G_i^{\ddagger} = \Delta H_i^{\ddagger} - T\Delta S_i^{\ddagger}$, respectively. In eq 8 C_{fi}, $i = 1, 2$ denote configurational factors almost independent of temperature T, $R = k_B N_A$ is the gas constant, and N_A is the Avogadro number. It is only briefly mentioned that $\Delta G_i^{\ddagger}$, $\Delta H_i^{\ddagger}$, and $\Delta S_i^{\ddagger}$ refer to molecular processes and, therefore, should be calculated from the dipole rotational correlation times[8]

$$\tau_{ri} < \tau_i \qquad i = 1, 2 \tag{9}$$

rather than from the dielectric relaxation times τ_i. Here we are interested in the activation enthalpies $\Delta H_i^{\ddagger}$ only, which remain almost unaltered when τ_{ri} is exchanged for τ_i, $i = 1, 2$. For this reason, as common practice, we simply use the τ_i values as following from the dielectric spectra (Table 3) in the discussion of the activation process.

As shown by Figure 9, the relaxation times τ_2 for C_6OH and for the mixture with mole fraction $x = 0.36$ of ethanol follow the Eyring behavior as predicted by eq 8. The τ_2 data for the ethanol-rich mixtures are too uncertain to allow for a clear conclusion on their dependence upon T. The plots in Figure 9 yield $\Delta H_2^{\ddagger} = (11.1 \pm 0.5)$ kJ/mol for C_6OH, $x = 0$, and $\Delta H_2^{\ddagger} = (6.7 \pm 1.3)$ kJ/mol for the mixture, $x = 0.36$. The finding of the activation enthalpy $\Delta H_2^{\ddagger}$ to increase with alkyl group concentration will be discussed in more detail below where the series of $\Delta H_1^{\ddagger}$ data for the low frequency relaxation is considered.

Within the framework of the wait-and-switch model, the high frequency relaxation process may be attributed to the reorientational motions of single hydrogen bonded dipolar groups within the chainlike alcohol molecular network. Computer simulations show that about 14% of the alcoholic OH-groups are involved in one H-bond only (C_1OH: 16.7%,[44] 16.5%;[46] C_2OH: 14.7%,[43] 14%;[47] C_3OH: 14.2%[43]). Hence the concentra-

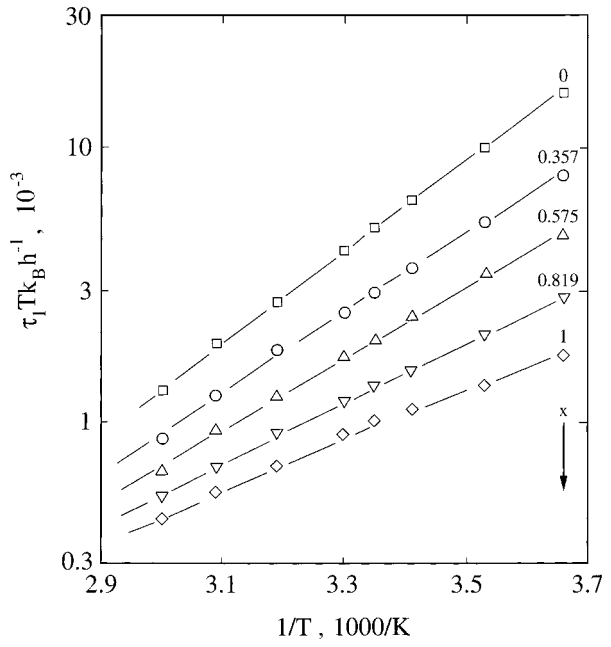

Figure 10. Eyring plot for the relaxation times τ_1 of the low frequency relaxation process for ethanol/*n*-hexanol mixtures with mole fraction *x* of ethanol.

TABLE 4: Activation Enthalpies for the Dominating Dielectric Relaxation of the Ethanol/*n*-Hexanol Mixtures at Room Temperature

x	$\Delta H_1^{\ddagger}$ kJ/mol
0	31.6 ± 0.4
0.357	27.6 ± 0.5
0.575	24.8 ± 0.4
0.819	20.9 ± 0.3
1	17.6 ± 0.6

tion of such sites is small and so is the relaxation amplitude $\Delta\epsilon_2$. On the other hand, there is a high content of sites (77%[43]) in which double hydrogen bonded OH-groups offer an additional neighbor for the formation of a new H-bond. Hence the period, for which the single-H-bonded dipolar group has to wait, until an appropriate partner for a new bond is available is rather small. As a consequence, the dielectric relaxation time τ_2 is rather small.

4.5. Low Frequency (Dominating) Relaxation. If the argumentation of the preceding section is accepted then the low frequency relaxation must be due to the waiting until the switching of double H-bonded dipolar groups into a new direction. Since there exists a high concentration of double hydrogen bonded OH-groups (77%) the relaxation amplitude $\Delta\epsilon_1$ ($> \Delta\epsilon_2$) of this process is large. Because only a comparatively small amount of single bonded OH-groups (14%) is available to serve as an additional neighbor for the formation of a new hydrogen bond, the period, that a given double-H-bonded molecule has to wait for suitable conditions for the switching process, is expected to be long. Hence τ_1 is larger than τ_2.

As shown by Figure 10, the relaxation time τ_1 of the ethanol/*n*-hexanol mixtures also follows an Eyring-type dependence upon temperature (eq 8). The slopes of the linear $ln(\tau_1 T k_B/h)$ vs T^{-1} relations yield activation enthalpies $\Delta H_1^{\ddagger}$ between 17.6 kJ/mol (C_2OH, $x = 1$) and 31.6 kJ/mol (C_6OH, $x = 0$). The finding of the $\Delta H_1^{\ddagger}$ values of the mixtures to monotonously increase with the hexanol concentration (Table 4) suggests that the activation enthalpy is not only given by the energy of the OH-group hydrogen bonding but that it contains also contributions from intermolecular interactions between $-CH_2-$ and $-CH_3$ groups. Evidence from infrared spectroscopy supports this suggestion as it reveals no change of the H-bond energy within the series of normal alcohols.[48] We therefore tentatively describe the molar enthalpy of activation $\Delta H_1^{\ddagger}$ of normal alcohols C_nOH by a sum of three terms

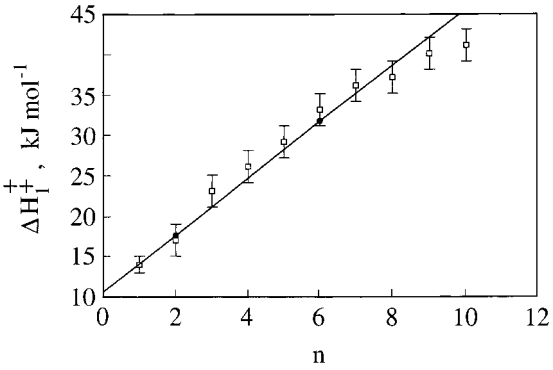

Figure 11. Activation enthalpies $\Delta H_1^{\ddagger}$ of the dominating (low frequency) relaxation process in normal alcohols C_nOH versus *n*. Full symbols indicate our data for ethanol and *n*-hexanol, open symbols represent data from the literature.[26] The line is the graph of eq 10 with $\Delta H_{CH_2}^{\ddagger} = 3.5$ kJ/mol from eq 11 and $\Delta H_{OH}^{\ddagger} + \Delta H_{CH_3}^{\ddagger} = 14.1$ kJ/mol from eq 12.

$$\Delta H_1^{\ddagger} = \Delta H_{OH}^{\ddagger} + (n-1)\Delta H_{CH_2}^{\ddagger} + \Delta H_{CH_3}^{\ddagger} \qquad (10)$$

Using our $\Delta H_1^{\ddagger}$ data for ethanol and *n*-hexanol, $\Delta H_{CH_2}^{\ddagger}$ can be calculated and also the activation enthalpies $\Delta H^{\ddagger}(C_nOH)$ for methanol ($n = 1$) and for the higher normal alcohols ($n = 2, ...$)

$$\Delta H_{CH_2}^{\ddagger} = {}^1/_4(\Delta H_1^{\ddagger}(C_6OH) - \Delta H_1^{\ddagger}(C_2OH)) \qquad (11)$$

$$\Delta H_1^{\ddagger}(C_1OH) = {}^1/_4(5\Delta H_1^{\ddagger}(C_2OH) - \Delta H_1^{\ddagger}(C_6OH)) \qquad (12)$$

$$\Delta H_1^{\ddagger}(C_nOH) = {}^1/_4((6-n)\Delta H_1^{\ddagger}(C_2OH) + (n-2)\Delta H_1^{\ddagger}(C_6OH)) \qquad n = 2, ... \qquad (13)$$

In Figure 11 $\Delta H_1^{\ddagger}(C_nOH)$ data resulting from our activation enthalpies for ethanol and hexanol are displayed as a function of *n*. Also shown are experimental $\Delta H_1^{\ddagger}$ values from the literature.[26] It is found that at $3 \le n \le 7$ the literature values somewhat exceed those predicted by our measurements, whereas at $n \ge 8$ the experimental activation enthalpies are somewhat smaller than calculated according to eq 13. Obviously, folding of the hydrocarbon chains of the higher alcohols results in a small reduction of the intermolecular interactions between the aliphatic groups and thus in a small negative curvature in the experimental $\Delta H_1^{\ddagger}$ vs *n* relation. In addition, a small effect of temperature may have been ignored here. The experimental $\Delta H_1^{\ddagger}$ data from ref 26 have been derived from relaxation times τ_1 at 150, 200, and 300 K, presupposing constancy of the activation enthalpy in this temperature range.

In conclusion, at $n \le 8$ the relaxation time of the dominating dielectric relaxation of normal alcohols may be well described assuming a rate process that is controlled by an activation enthalpy according to eq 10. Within the framework of this model the enthalpy contribution from a $-CH_2-$ group turns out to be $\Delta H_{CH_2}^{\ddagger} = 3.5$ kJ/mol which is a quite reasonable value. The finding of an additivity relation (eq 10) for the activation enthalpy again points at the important role of the aliphatic groups in the dielectric relaxation process. The approach of a single

H-bonded alcohol molecule to a site where it acts as the additional neighbor in the reorientation process is governed by diffusion and thus by the molecular size. The approach of a single H-bonded molecule to a double H-bonded site that acts as an additional neighbor is expected to likewise depend on the overall size of the molecules involved. In conformity with these expectations, $\Delta H_2^{\ddagger}$ decreases when ethanol is added to *n*-hexanol. The finding of the dielectric relaxation times τ_1 and τ_2 to distinctly exceed the life times of the H-bonds and of the H-bonding states of the OH-groups (from computer simulation for C_1OH[44]) may, in parts, be also due to the fact that in switching of a COH group from one to another H-bond the COH-rotation is possible only around a C-O bond or an H-bond as temporarily fixed axis. So the axial component of the COH− dipole vector remains unchanged in one switching step and, therefore, the variation of all dipole vector components is possible only after several waiting/switching periods.

References and Notes

(1) Tanaka, H.; Ohmine, I. *J. Chem. Phys.* **1987**, *87*, 6128.
(2) Ohmine, I.; Tanaka, H.; Wolynes, P. G. *J. Chem. Phys.* **1988**, *89*, 5852.
(3) Sciortino, F.; Fornili, S. L. *J. Chem. Phys.* **1989**, *90*, 2786.
(4) Ohmine, I.; Tanaka, H. *Chem. Rev.* **1993**, *93*, 2545.
(5) Geiger, A.; Mausbach, P.; Schnitker, A. In *Water and Aqueous Solutions;* Neilson, G. W., Enderby, J. E., Eds.; Hilger: Bristol, 1986; p 15.
(6) Sciortino, F.; Geiger, A.; Stanley, H. E. *J. Chem. Phys.* **1992**, *96*, 3857.
(7) Sagal, M. W. *J. Chem. Phys.* **1962**, *36*, 2437.
(8) Kaatze, U.; Pottel, R. *J. Mol. Liq.* **1992**, *52*, 181.
(9) Göttmann, O.; Kaatze, U.; Petong, P. *Meas. Sci. Technol.* **1996**, *7*, 525.
(10) Kaatze, U.; Pottel, R.; Wallusch, A. *Meas. Sci. Technol.* **1995**, *6*, 1201.
(11) Garg, K. S.; Smyth, C. P. *J. Phys. Chem.* **1965**, *69*, 1294.
(12) Crossley, J. *Adv. Mol. Relax. Processes* **1970**, *2*, 69.
(13) Jakusek, E.; Sobczyk, L. In *Dielectric and Related Molecular Processes;* Davies, M., Ed.; The Chemical Society: London, 1977; Vol. 3, p. 108.
(14) Gestblom, B.; Sjöblom, J. *Acta Chem. Scand.* **1984**, *A38*, 47.
(15) Gestblom, B.; Sjöblom, J. *Acta Chem. Scand.* **1984**, *A38*, 575.
(16) Kaatze, U.; Schäfer, M.; Pottel, R. *Z. Phys. Chem.* **1989**, *165*, 103.
(17) Barthel, J.; Bachhuber, K.; Buchner, R.; Hetzenauer, H. *Chem. Phys. Lett.* **1990**, *165*, 369.
(18) Barthel, J.; Buchner, R. *Pure Appl. Chem.* **1991**, *63*, 1473.
(19) Kaatze, U.; Schumacher, A.; Pottel, R. *Ber. Bunsen-Ges. Phys. Chem.* **1991**, *95*, 585.
(20) Buchner, R.; Barthel, J. *J. Mol. Liq.* **1992**, *52*, 131.
(21) Marquardt, D. W. *J. Soc. Indust. Appl. Math.* **1963**, *2*, 2.
(22) Petong, P., Diploma-Thesis, Georg-August-Universität, Göttingen, 1996.
(23) Atkins, P. W. *Physical Chemistry;* Oxford University Press: Oxford, 1978.
(24) Tanford, C. *The Hydrophobic Effect: Formation of Micelles and Biological Membranes;* Wiley-Interscience: New York, 1980.
(25) Ortega, J. *J. Chem. Eng. Data* **1982**, *27*, 312.
(26) Mandal, H.; Frood, D. G.; Saleh, M. A.; Morgan, B. K.; Walker, S. *Chem. Phys.* **1989**, *134*, 441.
(27) Powles, J. G. *J. Mol. Liq.* **1993**, *56*, 35.
(28) Ackadov, Y. Y. *Dielectric Properties of Binary Solutions;* Pergamon: Oxford, 1981.
(29) Landolt, H.; Börnstein, R., Eds. *Zahlenwerte und Funktionen aus Naturwissenschaften und Technik - Neue Serie, 2. Eigenschaften der Materie,* 6th ed.; Springer: Berlin, 1971.
(30) Buckley, F.; Maryott, A. A. *Tables of Dielectric Dispersion Data for Pure Liquids and Dilute Solutions;* NBS Circular 589, National Bureau of Standards: Washington DC, 1958.
(31) Fröhlich, H. *Theory of Dielectrics;* Clarendon: Oxford, 1958.
(32) Hill, N. E. In *Dielectric Properties and Molecular Behaviour;* Hill, N. E., Vaughn, W. E., Price, A. H., Davies, M., Eds.; Van Nostrand Reinhold: London, 1969.
(33) Kirkwood, J. G. *J. Chem. Phys.* **1939**, *7*, 911.
(34) Böttcher, C. J. F. *Theory of Electric Polarization. 1. Dielectrics in Static Fields;* Elsevier: Amsterdam, 1973.
(35) Shinomiya, T. *Bull. Chem. Soc. Jpn.* **1989**, *62*, 908.
(36) Shinomiya, T. *Bull. Chem. Soc. Jpn.* **1989**, *62*, 2258.
(37) Kaatze, U. *J. Chem. Eng. Data* **1989**, *34*, 371.
(38) Hill, N. E. *J. Phys. C: Solid State Phys.* **1970**, *3*, 238.
(39) Akerlöf, G. *J. Am. Chem. Soc.* **1932**, *54*, 4125.
(40) Jordan, B. P.; Sheppard, R. J.; Szwarnowski, S. *J. Phys. D: Appl. Phys.* **1978**, *11*, 695.
(41) Krishnaji, V.; Agarwal, V. K.; Kumar, P. *J. Chem. Phys.* **1972**, *56*, 5034.
(42) Davidson, D. W.; Cole, R. H. *J. Chem. Phys.* **1950**, *18*, 1417.
(43) Jorgensen, W. L. *J. Chem. Phys.* **1986**, *90*, 1276.
(44) Debus, A. Diploma-Thesis, Georg-August-Universität, Göttingen, 1996.
(45) Eisenberg, D.; Kauzmann, W. *The Structure and Properties of Water;* Clarendon: Oxford, 1969.
(46) Padró, J. A.; Saiz, L.; Guàrdia, E. *J. Mol. Struct.* **1997**, *416*, 243.
(47) Saiz, L.; Padró, J. A.; Guàrdia, E. *J. Phys. Chem. B* **1997**, *101*, 78.
(48) Wilson, L.; Bicoa De Atencastro, R.; Sandorfy, C. *Can. J. Chem.* **1985**, *63*, 40.